

# Using Natural-Product-Based Treatments, Such as Polymer Loaded with Ginger for the Management of Osteochondral Disorder

G. Ben Salah

\* G.SALAH@qu.edu.sa

Department of pharmacology and toxicology, College of Pharmacy, Qassim University, Al Qassim, Saudi Arabia

Received: November 2023

Revised: July 2024

Accepted: September 2024

DOI: 10.22068/ijmse.3429

**Abstract:** This study reported the biological changes occurring after  $\gamma$ -irradiation of *in vivo* rat model and the osteochondral protective effect of Gelatine-Chitosan-Ginger (GEL-CH-GING). The results indicated that Electron Paramagnetic Resonance (EPR) Spectroscopy of GEL-CH-GING identified two paramagnetic centers with g-values of 2.19 and 2.002. Fourier Transform Infrared Spectroscopy (FTIR) analysis demonstrated an increased intensity in the peaks corresponding to C-H chains and C=O carbonyl groups. Additionally, X-ray Diffraction (XRD) analysis revealed no alteration in crystallinity. After gamma ray exposure, the rat groups have received an osteochondral defect and then were treated with GEL-CH-GING composite. Sixty days post-surgery, a significant reduction in thiobarbituric acid-reactive compounds (TBARs) was seen when compared to non-implanted rat group. Concerning oxidative stress status, GEL-CH-GIN significantly improved Superoxide Dismutase (SOD) 76 nmol/l, Catalase (CAT) 0.79 nmol/l, and Glutathione Peroxidase (GPx) 1.77 nmol/l activities in osteochondral tissue. Regarding the histomorphometric parameters of cartilaginous tissue (nCg.Th,  $\mu\text{m}$ ), (cCg.Th,  $\mu\text{m}$ ), (Cg.Th,  $\mu\text{m}$ ), irradiated-GEL-CH-GIN group showed a significant increase as compared to irradiated group with 116, 74 and 188  $\mu\text{m}$ , respectively ( $p < 0.01$ ). The microanalysis showed a high percentage of O and C in the regeneraed osteochondral tissue and indicated the deposition of novel collagen matrix. The biomechanical behaviour showed a significantly enhanced hardness measurement ( $1.73 \pm 0.029$  VH,  $p < 0.05$ ) when compared with that of irradiated group. Biochemical markers suggested an osteocartilage repair capacity. In fact, the levels of IL-1 $\beta$ , IL-6, TNF- $\alpha$  and VEGF in the implanted rat with GEL-CH-GING composite exhibited  $51 \pm 3.48$ ,  $30.05 \pm 5.18$ ,  $65.12 \pm 4.33$  and  $40.42 \pm 3.32$  ng/l, respectively. Our findings suggested that GEL-CH-GING composite might have promising potential applications for cartilage healing.

**Keywords:** Ginger,  $\gamma$ -irradiation, Biomaterial, Oxidative stress, Asteochondral defect.

## 1. INTRODUCTION

Irradiation may cause active deterioration and reduces matrix synthesis in bone and articular cartilage [1]. The effect of irradiation on proliferative chondrocytes illustrated the alterations in proliferation, cellular differentiation, and induction of chondrocyte apoptosis [2]. Irradiation of cartilaginous tissue enhanced proteoglycan degradation that might increase free radicals induction [3]. In fact, it has been reported that the oxidative stress derived from radiation exposure damages DNA and changes the amount and quality of cartilage cell [4]. Additionally, oxidative stress contributes to the production of inflammatory mediators like cytokines in chondrocytes [5]. Irradiation of cells increases the release of inflammatory cytokines, including IL-6, due to DNA damage signaling [6]. Failure in conventional treatment of cartilage diseases has led researchers to find alternatives in tissue engineering. Recently, researchers have explored the potential of biomaterials in treating

cartilage diseases. For this purpose, Chitosan (CH) is considered as a very attractive polymer and a poly-functional (poly amino-saccharide) with outstanding activities related to biodegradability, biocompatibility, antibacterial activity, low immunogenicity and controlled release behaviour [7-11]. However, the poor mechanical qualities of CH can cause hindrance to repair the damaged tissue. In fact, inadequate mechanical properties can delay the regeneration of damaged tissue and also may affect the cells viability which suggests the significance of selecting appropriate biomaterials as scaffolds for cell adhesion and proliferation.

The gelatine (GEL), a collagen-derived substance, has been shown to have attractive mechanical properties associated with the biocompatible properties with cartilaginous tissues [12, 13]. GEL does not trigger any immune response in the human body [14]. It is made up of proline, hydroxyproline and glycine which help cells to join together [15]. Both CH and GEL serve as polymeric cartilage materials

increasing the stability of some bioactive substance such as polyphenol extract. In fact, this latter substance incorporation serves to protect cartilage from gamma rays due to its possessing antioxidant and anti-inflammatory properties.

Among the natural extracts rich in bioactive compounds, ginger (GING) is considered as a complex of bioactive elements such as, gingerols, shogaols, and parasols known by their anti-inflammatory activities [16]. In addition, GING extract efficiently inhibits the expression of cytokines, such as TNF- $\alpha$ , interleukin-6, and interleukin-8 mRNA rate. Moreover, GING significantly inhibited the production of NO and prostaglandin E-2 in cartilage tissue, which approve reducing cartilage inflammations and degradation [17].

Here, the impact of gamma irradiation on osteochondral defect was studied using *in vivo* rat model. As an alternative therapy for cartilaginous disorder, an innovative GEL-CH-GING composite was formulated and grafted as a promising therapeutic implant. To the best of our knowledge, biopolymers based GING extract has been explored for the first time to generate new osteocartilaginous tissue.

## 2. MATERIALS AND METHODS

### 2.1. Preparation of GEL-CH-GING Composite

A GEL solution with a concentration of 5.0 wt% was prepared by dissolving 5 g of GEL powder in 100 ml of distilled water for 30 minutes, followed by heating at 50°C for 30 minutes while continuously stirring. CH (85% degree of deacetylation) was obtained from a pharmacy in Tunisia. Ginger (*Zingiber Officinale*) extract was dissolved in a 2% w/w ethanolic solution and then gently added to the GEL solution. The resulting mixtures was warmed and stirred at 50°C for 30 minutes to ensure uniformity. Finally, the mixture underwent repetitive freeze-thawing for four cycles to complete the preparation.

### 2.2. Sterilization of GEL-CH-GING Composite

The GEL-CH-GING composite was irradiated at a Cobalt-60 gamma irradiation facility with energy levels of 1.173 and 1.332 MeV and a dose rate of 36 Gy/min. The dose rate was measured using a Fricke dosimeter, a chemical standard dosimeter. Traceability to the Secondary Standard Dosimetry Laboratory (SSDL) was ensured using

the Alanine/EPR dosimetry system. The composite was placed in a polystyrene phantom to maintain electronic equilibrium and was irradiated at room temperature (293–298 K) with a dose of 15 kGy.

### 2.3. Electron Paramagnetic Resonance (EPR) Spectroscopy

The electron paramagnetic resonance (EPR) spectra of the composite samples were recorded at room temperature on a Bruker ER-200D spectrometer operating at 9.8 GHz X-Band frequencies with modulation amplitude of 0.2 mT, modulation frequency of 100 khz, sweep width of 210 mT and microwave power of 63 mW.

### 2.4. The X-ray Diffraction (XRD)

The X-ray diffraction analysis of the composites were conducted using Brucker D8 advance with Cu-K $\alpha$  radiation of wavelength  $\lambda = 1.541 \text{ \AA}$  in 20 values in the range of 15–90°. The results obtained by X-ray measurement were analyzed with the X'PertHigh Score Plus program.

### 2.5. Fourier Transform Infrared (FTIR) Spectroscopy

The Fourier transform infrared (FTIR) spectroscopy is used to study the structural and chemical properties of the composites. The measurement was recorded by Vertex 70 infrared spectrometer from 4000 to 400  $\text{cm}^{-1}$  at a spectral resolution of 2  $\text{cm}^{-1}$  and 32 scans

### 2.6. Rats Manipulation and Ethical Considerations

Fourty male Wistar rat (15–16 weeks old) from the Central Animal House were utilized for the study. They were provided with unrestricted access to water (Mica, Tunisia) and were maintained in a controlled environment with standard temperature and humidity levels (22  $\pm$  2°C and 55  $\pm$  5 percent, respectively), along with a 12-hour light/dark cycle. Prior to the experiment, all rats underwent a one-week acclimatization period. The rats were monitored daily for clinical lameness or other complications. This study adhered to the guidelines set by the National Center for Sciences and Nuclear Technologies (Tunisia), following the "Guide for the Care and Use of Laboratory Animals," and was approved by the local Ethics Committee of the Laboratory of Energy and Matter Research Laboratory (LR16CNSTN02).

## 2.7. Protocol of Rat Gamma-Ray Exposition

Anesthesia was induced with 10 mg/kg of ketamine (Ketaminol, Intervet International GmbH, Unterschleißheim, Germany) and 0.1 mg/kg of Xylazine (Rompun, Bayer Healthcare, Puteaux, France). Supplemented local anesthesia was applied after 25 min using 4 mg/kg carprofen (Rimadyl, Pfizer, France). Irradiation with gamma ray was established with anterior and posterior areas of photons with Cobalt 60. The dosimetric measurements for rats were performed by using a scanner. The animals were introduced in a filled packet to guarantee dose homogeneity throughout the interest area. Varian Eclipse software was used to estimate the doses of 1.5 Gy of 60 Co radiations in the osteochondral level in order to validate the irradiation technique. All rats were arbitrarily divided into 4 different groups with (6 animals per group) (Figure 1)

## 2.8. Surgical and Postoperative Protocols

Articular osteo-cartilaginous tissues were used as the recipients of the GEL-CH-GING composite. Right stifle joint was exposed by medial parapatellar arthrotomy after skin preparation and sterilizing, and the patella was subluxed to enable full exposure of the stifle joint. A chondral defects, 2 mm in diameter and 2 mm in height, were introduced in medial and lateral femoral condyles. The GEL-CH-GING composite were implanted into the defect area over the medial femoral condyle. After implantation into the defects, the composite re-expanded due to the influx of fluid from bone marrow and joints and fit the chondral defect site firmly.

## 2.9. Tissue Preparation and Oxidative Stress Assessment

### a. Measurement of Thiobarbituric Acid-Reactive Substances (TBARS)

The cartilaginous tissues were removed and quickly frozen by dry ice. The tissues from

each group were then minced, homogenized at 100 mg/ml, and centrifuged at 3,000 g for 15 minutes at 48°C in a 0.1 mol/l Tris-HCl buffer with a pH of 7.4. By testing TBARS, which are the end result of lipid peroxidation, the amount of lipid peroxidation in the tissue homogenate was calculated [18].

### b. Measurement of antioxidant enzymes

The activity of superoxide dismutase (SOD) was assessed using a spectrophotometer [19]. The technique used to evaluate the activity of glutathione peroxidase (GPx) is cited by Pagila and coll. [20]. The calorimetric measurement of catalase (CAT) activity at 240 nm was quantified as the number of moles of H<sub>2</sub>O<sub>2</sub> used per minute per milligram of protein [21]. The method of Lowry and coll. [22] was used to measure the total protein level using bovine serum albumin.

## 2.10. Hardness Measurement

Vickers Tester was used to gauge the hardness. The Vickers hardness (VH) number is given by the formula:  $H = 2P \sin(h/2)/D^2$ , where P is the applied load in kilograms, D is the average diagonal length in millimetres, and h is the angle (136°) between the Diamond Pyramid's. Measurements are taken following the composites cartilage implantation.

## 2.11. Histomorphometric Evaluation

The implanted osteocartilaginous tissue was removed, preserved in formalin (Burdack), and then chilled. The specimens were dehydrated with alcohol solutions ranging from 70% to 100% EtOH. After that, the specimens were immersed in a solution of methyl methacrylate (MMA) and glycol methacrylate (GMA), without first being decalcified, and allowed to polymerize. Sections of 6-7 mm thick were produced using a sliding microtome (Reichert-Jung) by cutting along a transverse plane.

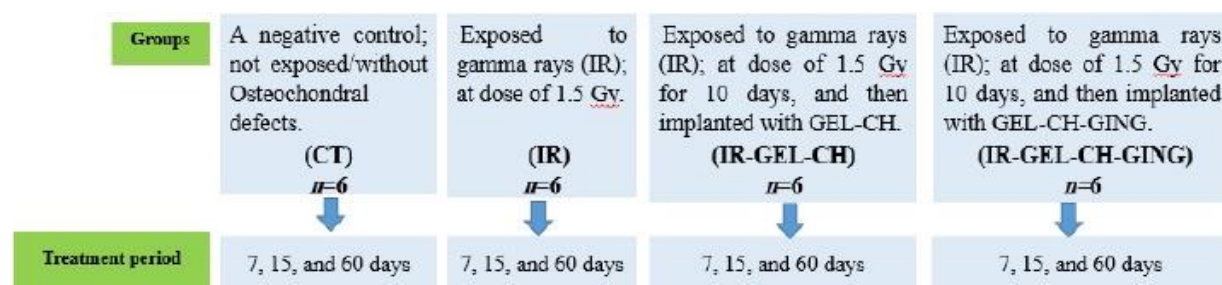


Fig. 1. Experimental protocol

The sections were also stained using a modified Goldner trichrome. The histomorphometric parameters were assessed using a 25-point integrating filter and the point count method [23]. From the histological zones of the implanted cartilage tissue, the subsequent parameters of cartilage thickness were determined independently and expressed as mean distances: 1-Non-calcified cartilage thickness (nCg.Th). 2-The calcified cartilage thickness (cCg.Th). 3-Total cartilage thickness (CgTh).

## 2.12. Measurement of Biochemical Biomarker in Serum

Venous blood draws were performed to acquire serum, which was then utilized to quantify the levels of IL-1, IL-6, TNF-, and VEGF by ELISA in accordance with the manufacturer's recommendations.

## 2.13. Microanalysis of Implanted Osteochondral Tissues

The microanalysis of the implanted osteochondral tissues samples were investigated using a FEI Quanta 200 environmental scanning electron microscope (SEM) coupled with EDAX and operating at 20 kV. The GEL-CH-GING implanted cartilage were initially fixed in a 2.5% glutaraldehyde solution (phosphate buffer, pH 7.3) overnight, followed by washing with a phosphate buffer solution (pH 7.4). Next, the samples were post-fixed in a 2% acid solution (phosphate buffer solution (pH 7.4) for 90 minutes and then dehydrated using an alcohol evaporation system. The grafted tissues were subsequently freeze-dried using a freeze-dryer.

## 2.14. Statistical Analysis

All measurements are reported as means ( $n= 6$ )  $\pm$  standard deviations (SD). Multiple comparisons were conducted using analysis of variance (ANOVA) followed by Tukey's range test. A  $p$ -value  $< 0.05$  was considered significant.

## 3. RESULTS

### 3.1. Electron Paramagnetic Resonance (EPR) Analysis

EPR detects unpaired electrons, such as the ones present in free radicals (Figure 2). When GEL-CH-GING composite was irradiated with the aim of being sterilized, free radicals are generated,

from the main signal and were associated with the radicals produced by irradiation in polymer composite. Non-irradiated samples reveals two EPR signals with a  $g$  factor of 2.004 and 2.009 ascribed to free radicals and were associated with the radicals produced in GING cellulose containing powder [24]. Whereas in irradiated samples exhibit only one central singlet EPR signal whose intensity decreased upon irradiation with the degenerescence of the two side peaks that induced next polymer irradiation.

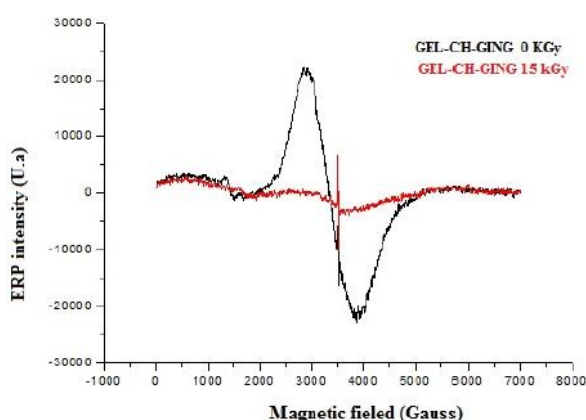


**Fig. 2.** EPR spectrum of sterilized GEL-CH-GING composite with 15 kGy in comparison with control samples (0 kGy).

### 3.2. Fourier Transform Infrared (FTIR) of GEL-CH-GING Omposite

FTIR spectrum of control and sterilized composite with 15 kGy gamma rays dose were signalled at the absorption region of 400–4000  $\text{cm}^{-1}$ . It is related to the tensile vibrations of the acid hydroxyl groups of GING and amine of the CH and GEL polymeric bed. In this vibration region, a band at about 3436  $\text{cm}^{-1}$  can be the result of the hydrogen bonding formation between the GING structures and polymeric bed in the formulated composite. The bands at 784  $\text{cm}^{-1}$  are attributed to N-H were more accentuated for the irradiated composite. The characteristic band of the transformed groups does not detect any new bands which confirm to the constriction of hydrogen bonding stretch after irradiation (Figure 3).

### 3.3. X-ray Diffraction (XRD)

The XRD pattern displayed distinct peaks corresponding to the control and sterilized composite GE-CH-GING (Figure 4). The XRD pattern of GEL powder exhibited an amorphous

morphology with a broad hump characteristic of the range 15-30 (20). These peaks are typically associated with the triple helical crystalline structure of GEL [25]. In contrast, the XRD pattern of CH showed a sharp crystallographic peak at 22 (20) [26].

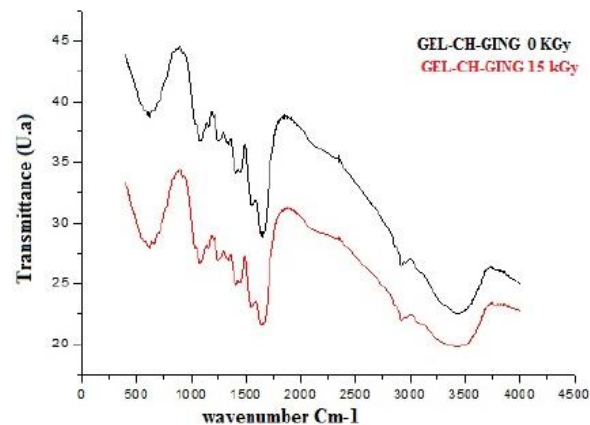


**Fig. 3.** FTIR spectrum of sterilized GEL-CH-GING composite with 15 kGy in comparison with control samples (0 kGy).

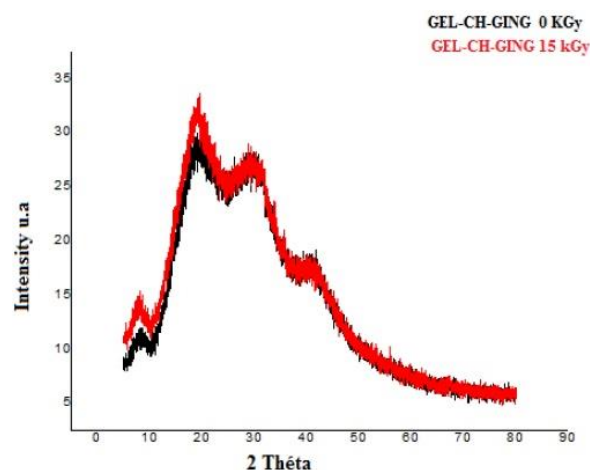


**Fig. 4.** X-ray diffractograms of sterilized GEL-CH-GING composite with 15 kGy in comparison with control samples (0 kGy).

The amorphous structure of GING cellulose also signaled a peak at around 38 (20) [27]. Peak intensity did not change significantly and the crystallinity of cellulose was not disrupted at large. Irradiation at 15 kGy did not transform amorphous structure via the breaking of intermolecular chemical bonds. Also, no new functional peaks of semi-crystalline composite were appeared.

#### 3.4. Oxidative Damage in Cartilage Tissue

The evaluation of the oxidative stress biomarker

as well as the antioxidant enzyme activity after the GEL-CH-GING implantation in the articular osteochondral tissue are shown in Figure 5. MDA level in the osteochondral tissue following 7 days of graft were significantly different when compared with that of control CT ( $p < 0.05$ ). CAT, SOD, and GPx activities in the rat osteochondral tissue exhibited a highly significant decline when compared with those of CT rat tissues ( $p < 0.05$ ). However, after 60 days of biomaterial implantation, a significant enhanced enzyme activities were observed in the regenerated tissue when compared with those of IR group ( $p < 0.05$ ). In fact, the SOD, CAT and GPx activities in osteochondral tissue, showed 76, 0.79, and 1.77 nmol/l, respectively.

#### 3.5. Histological Analysis

The formulated implant is adapted for implantation at an osteochondral site to promote the growth or formation of cartilaginous tissue (Figure 6a). To assess the biomaterial effect on the osteochondral property, the explanted grafts were examined by histological analysis 60 days post-surgery. The GEL-CH-GING composite induce newly osteocartilagenous formed tissue with a marginal spreading cells (Figure 6b). The GEL-CH-GING grafts showed similar outcomes comparable to the control 60 days post-surgery (Figure 6d), the development of the graft towards hyaline was detected without body inflammatory reaction due to the safety of the polymeric implant. This result is associated to the biocompatibility of this biomaterial and the capacity to enhance cartilage remodelling. As shown, the synthesized composite enhanced chondrogenesis that favour surface cell configuration and high cell density (Figure 6h). Histologically, a matrix-rich tissue with uniform cell distribution could be demonstrated. The staining showed the deposition of homogenous distributed proteoglycans within the matrix (Figure 6l). After 60 days, the grafts showed a positive collagen fibril assembly surrounding cells and proteoglycans.

#### 3.6. Histomorphometric Evaluation

Histomorphometric analysis data are shown in Table 1. After 15 and 30 days of implantation, no amelioration of the histomorphometric parameters (nCg.Th, cCg.Th and Cg.Th) were detected. However After 60 days of implantation, the

condylar cartilage compartments showed a significant increase of all parameters in the injured sites of cartilaginous tissues compared to that of IR rat group. In fact, the parameters nCg.Th,  $\mu\text{m}$ , cCg.Th,  $\mu\text{m}$  and Cg.Th in the irradiated-GEL-CH-GIN group showed a

significant increase as compared to irradiated group with 116, 74 and 188  $\mu\text{m}$ , respectively ( $p < 0.01$ ). So, the GEL-CH-GING composite have the capacity to reconstruct the cartilage thickening found when comparing with the untreated-control group.

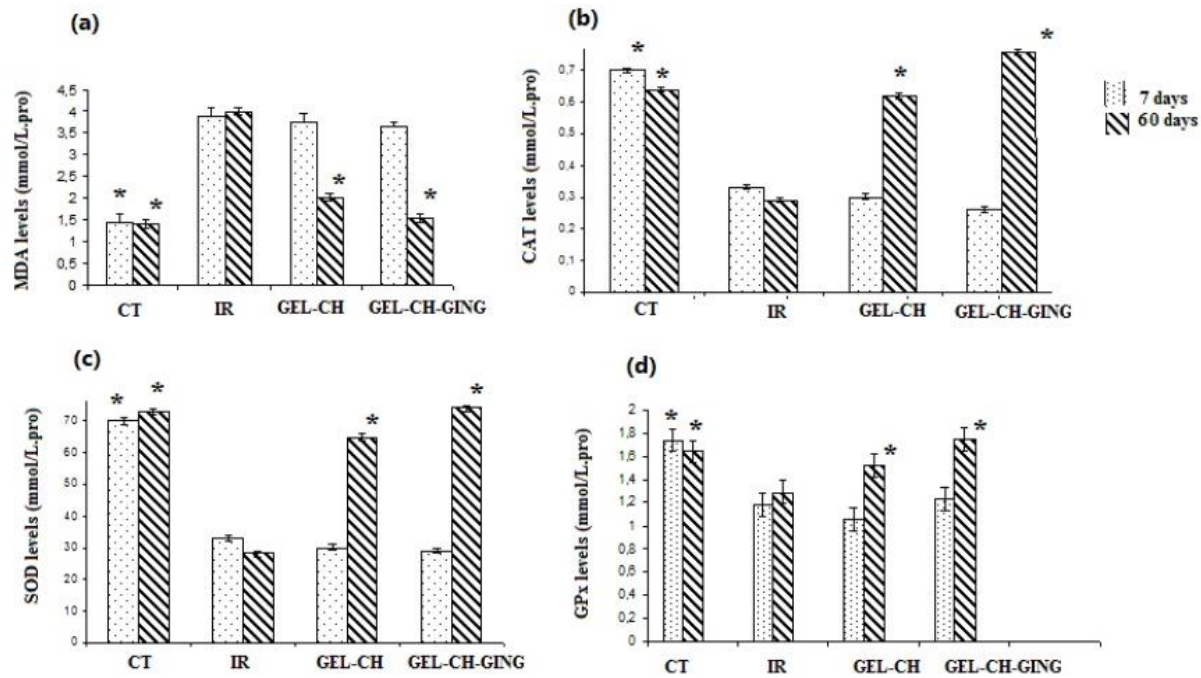


**Fig. 5.** Effects of GEL-CH-GING composite on MDA levels (a) CAT (b), SOD (c) and GPx (d). \* Highly statistically significant ( $p < 0.01$ ) as compared to the irradiated group (IR).

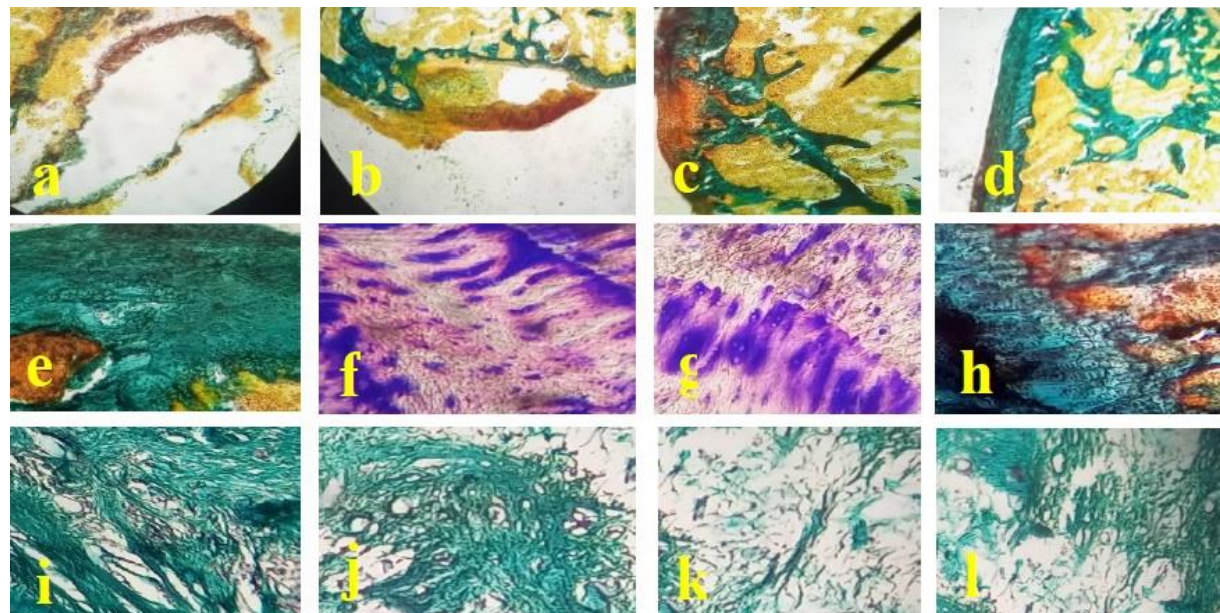


**Fig. 6.** Histological analysis of the implanted cartilage. a: Biomaterial, b: Implanted cartilage 7 day post-surgery, c and d: Regenerated cartilage 15 and 60 days post-surgery, respectively. e: Chondrocyte of the control cartilage. f, h, and h: Chondrocytes of cartilage tissue after 7, 15 and 60 days of implantation, respectively. i, j, k, and l: Regenerated collagen in the control, cartilage tissue after 7, 15, and 60 days of implantation, respectively.

**Table 1.** Histomorphometric analysis of grafted articular cartilage after 7, 15, and 60 days.

	nCg.Th (μm)			cCg.Th (μm)			Cg.Th (μm)		
	7d	15d	60d	7d	15d	60d	7d	15d	60d
CT	109±51	111±33	111±49	76±23	78±13	77±33	181±55	184±43	185±43
IR	87±24	80±22	77±21	66±23	60±15	59±26	150±34	139±44	130±43
GEL-CH	120±44	117±55	115±32	96±19	91±22	80±15	212±65	210±54	192±43
GEL-CH-GING	124±32*	119±65*	116±23*	85±15	81±20*	74±21*	202±45*	202±33*	188±53*

nCg.Th: Non-calcified cartilage thickness, cCg.Th: Calcified-cartilage thickness, Cg.Th: Total cartilage thickness of the sterilized GEL-CH-GING composite rat, IR: irradiated rat group, CT: control group. \*Highly statistically significant ( $p < 0.01$ ) as compared to the irradiated group (IR).

### 3.7. Microanalysis of Implanted Osteochondral Tissues

The results showed the mineral distribution in the implanted GEL-CH-GING composite 60 days post-surgery (Figure 7).

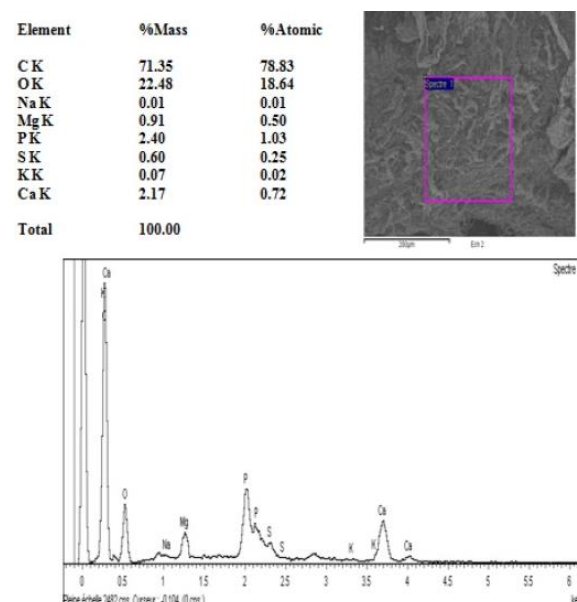


**Fig. 7.** EDX-Analysis of mineral composition of implanted cartilage with GEL-CH-GING composite 60 days post-surgery.

A high percentage of O and C were detected in the osteochondral tissue. The later indicate the novel deposition of an organic matrix made by collagen as described previously in Chen's study [28]. The presence of S may represent sulfate

groups in the organic matrix. In addition, in the regenerated cartilage the other element such as Na, K, Fe and Mg represent the release of the degraded and absorbed biomaterial in the irradiated rats.

### 3.8. Hardness Measurement

The Table 2 illustrates the measurements hardness of the implanted osteocartilaginous tissue after 7, 15, and 60 days. The IR-GEL-CH-GING implanted tissue hardness values exhibited a similar biomechanical behavior as compared to that of native condylar cartilage tissue. In fact, this mechanical property was increased progressively and went up to even higher levels after 60 days and it reached  $1.7 \pm 0.029$  Vicker's hardness (VH) in the IR-GEL-CH-GING treated cartilage rat.

### 3.9. Measurement of Biochemical Biomarker in Serum

The serum level measurements in the different treated rats are shown in Figure 8. The levels of IL-1 $\beta$ , IL-6, TNF- $\alpha$  and VEGF in the implanted rat with GEL-CH-GING composite were  $51 \pm 3.48$ ,  $30.05 \pm 5.18$ ,  $65.12 \pm 4.33$  and  $40.42 \pm 3.32$  ng/l, respectively. These values were decreased with statistically significant differences ( $p < 0.01$ ) as compared with IR rats. However these biomarkers never reach those of control because the irradiation concerned all the rat body.

## 4. DISCUSSION

**Table 2.** The measurement of hardness in the GEL-CH-GING composite rat irradiated group and native cartilage.

Animal group	7 days	15 days	60 days
CT	$1.77 \pm 0.09$	$1.75 \pm 0.071$	$1.76 \pm 0.59$
IR	$1.55 \pm 0.05$	$1.59 \pm 0.061$	$1.58 \pm 0.069$
GEL-CH	$1.22 \pm 0.091$	$1.63 \pm 0.054$	$1.66 \pm 0.065$
GEL-CH-GING	$1.44 \pm 0.066$	$1.66 \pm 0.086$	$1.73 \pm 0.029^*$

CT= control group, IR irradiation group, GEL-CH treated group, and GEL-CH-GING treated group. \*Statistically significant ( $p < 0.015$ ) as compared to the irradiated group (IR).

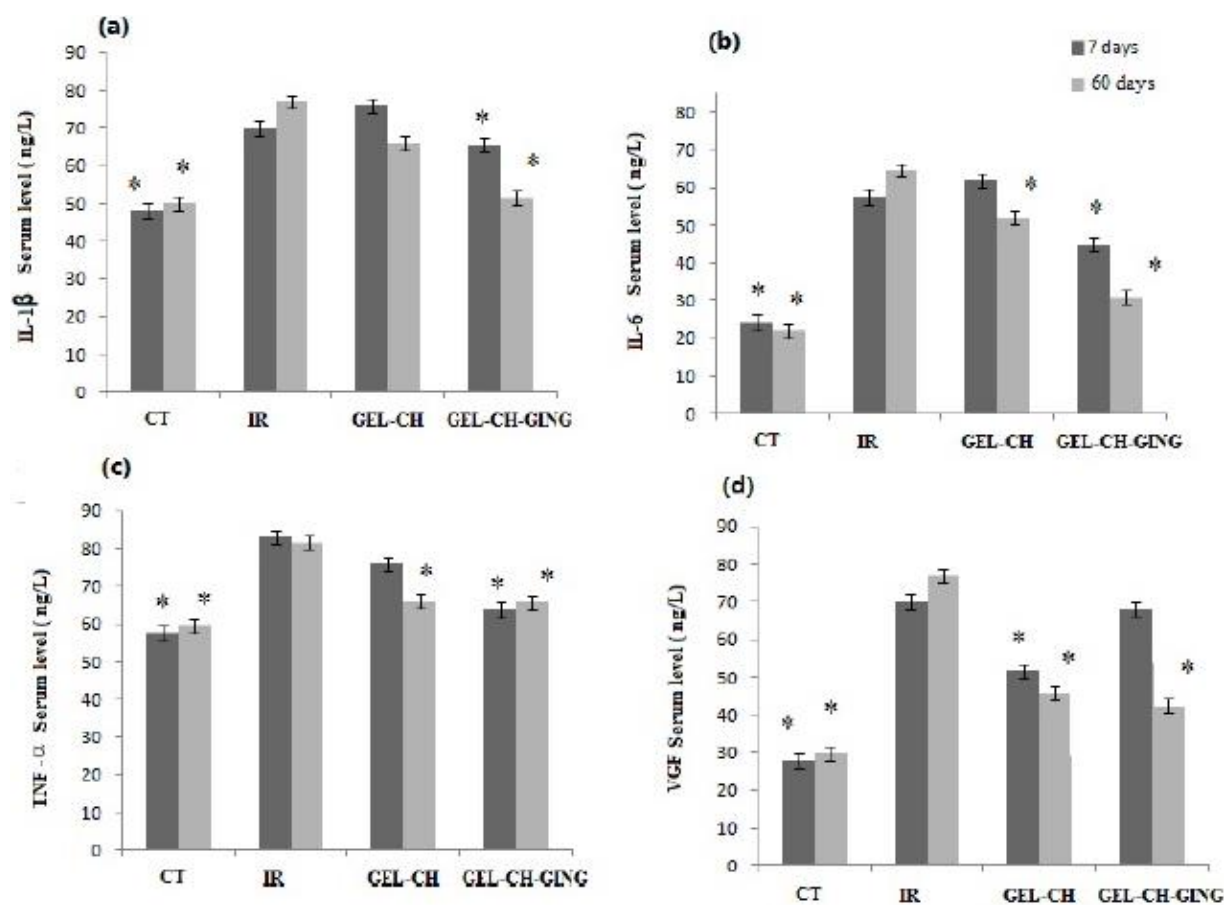


**Fig. 8.** Levels of interleukin-1 $\beta$  (a), interleukin-6 (b), tumor necrosis factor- $\alpha$  (c) and vascular endothelial growth factor (d) in treated and control groups in the GEL-CH-GING composite rats, GEL-CH rats, irradiated rats (IR) and control (CT) after 60 post-surgery. \*Highly statistically significant ( $p < 0.01$ ) as compared to the irradiated group (IR).

Polymers derived from natural sources have great potential for biomedical applications. In the current study, an innovative bioactive biopolymer based on GEL, CH and GING extract was developed and characterized for osteocartilagenous graft tissue.

To the best of our knowledge, no available studies explored the protective and antioxidant activity of natural polymer based GING against radiation induced harmful effects in the rat cartilage tissue. The physico-chemical analysis of the sterilized biomaterial exhibited an elevated peak signal assigned to GEL 15-30, 22 and 38 (20) for both CH and GING powders, respectively. After sterilization the angle locations of GING extract interacted with CH and Gel powders were unaffected. The results specified that there was no difference in the protein backbone structures as compared with non-sterilized composite. The peaks around 22.20 in the pattern proteins as noticed X-ray reflection belong to the  $\beta$ -sheet

structure [29]. For that it was suggested that a part of crystalline cellulose derived from GING was not disrupted by bending with CH and GEL matrix [29]. On the other hand, the EPR spectra of un-irradiated GEL-CH-GING and that treated with 15 kGy was shown a doublet signal, attributed to the presence of the radiation of the radicals derived from carbohydrate. So, the analysis showed the same composition, but with different intensity ratios of the central line assigned to cellulose radicals derived from GING [30].

Concerning FTIR spectrum, the intermolecular interactions between CH and functional groups of both GEL and GING extract were established. Different functional groups such as C=C aromatics content, -OH band at wavelength of  $1380\text{ cm}^{-1}$  were detected. The characteristic absorption bands corresponding to  $3284.92\text{ cm}^{-1}$  are due to the -OH groups of phenolic compounds and flavonoids present in GING and the CH and

GEL amine in the polymeric bed. FTIR spectrum results concluded that there was an interaction between CH, GEL matrix and GING extract during incorporation process. Moreover, the characteristic absorption bands corresponding to the vibration frequencies of  $1643.64\text{ cm}^{-1}$  are due to the carbonyl groups of phenolic compounds [31]. The characteristic absorption bands corresponding to the vibration frequencies of  $1084.86\text{ cm}^{-1}$  due to the OH bending of the phenolic compounds and flavonoids [32]. The bands at 784 are attributed to N–H derived from GEL matrix. However, there was no new peak significantly changed due to gamma sterilization. Containing various active functional groups, GEL-CH-GING may participate to diverse compounds which might be responsible for the various biological activities such as antioxidative phenomenon.

The rats group received ionizing radiation is subjected to the increased production of reactive oxygen species (ROS), and, as a result, an oxidative stress. Lipid peroxidation by TBARS test demonstrated that the irradiated group presents the highest level. This analysis is an attack of various cell components by free radicals leading to biochemical changes and macromolecule modifications [33, 34]. Thus, the present study demonstrated that harmful oxidative molecules such as MDA are produced during ionizing radiation reaction at 1.5 Gy of the whole body irradiation of rats.

ROS have a harmful effect on the cellular antioxidant defence mechanisms by falling the level of antioxidant enzymes in osteocartilaginous tissue, especially catalase (CAT), superoxide dismutase (SOD) and glutathione peroxidase (GPx). The formulated biomaterials contain natural antioxidants derived from GING that were applied to detoxify the increased levels of free radicals. In fact, after the GEL-CH-GING graft, the antioxidant mechanisms of the body were enhanced as shown by elevated cartilage GPx, SOD and CAT activities with reduction of cartilaginous MDA level.

These results might be attributed to the reaction between the free radicals and the free residual amino groups to form CH ammonium groups. In addition, it might be attributed to the anti-oxidative effect of phenolic compounds, such as quercetin, zingerone, gingerenone-A, and 6-

dehydrogingerdione [35]. Moreover, as described, GING extract contains several terpene components, such as  $\beta$ -bisabolene,  $\alpha$ -curcumene, zingiberene,  $\alpha$ -farnesene, and  $\beta$ -sesquiphellandrene known as very powerful antioxidant components [35]. Antioxidants function to reduce or stop these chain reactions by neutralizing free radicals or inhibiting other oxidative reactions [36].

On the other hand, our data revealed elevated serum level of IL-1 $\beta$ , IL-6, TNF- $\alpha$  and VEGF indicating that the irradiation induced inflammatory processes. This finding has been previously reported in Lee's study that demonstrated that irradiation marked up-regulation of mRNA and protein expression of the pro-inflammatory mediator TNF- $\alpha$  [36]. After GEL-CH-GING graft, these biomarkers were reduced but did not return to the normal level. This finding might be explained by the fact that the reparation is focusing in the focal areas of degenerated cartilage however the irradiation concerned all the body. Moreover, it has been reported that the bioactive ingredients in GING, such as gingerols, shogaols exert anti-inflammatory protective effects on chondrocytes and human synoviocytes by specifically decreasing the production of inflammatory mediators [37]. In addition, gingerol suppresses inflammatory degradation enzymes such as the nitric oxide (NO) synthase, which has been shown to be regulated and promoted by the master transcription factor NF- $\kappa$ B [37]. Also, GING suppress the expression of pro-inflammatory cytokines, such as TNF- $\alpha$ , interleukin-6, and interleukin-8 mRNA levels, thereby reducing cartilage inflammations and degradation [37].

The microanalysis of the implanted cartilage revealed that the organic matrix after remodelage and some of acid groups might possibly derived from sulfate groups of glycosaminoglycans obtained from CH. In fact, in cartilage matrix, virtually all the sulfur is found as sulfate in (Glycosaminoglycans) GAG [37, 38].

Additionally, it is well known that CH is composed of glucosamine and N-acetylglucosamine, with a structure and properties similar to GAG. Thus, CH provides a favorable microenvironment for native cells to adhere, colonize, and repair damaged tissue. However, it does not promote chondrocyte differentiation, proliferation, or matrix secretion [39].

The GEL-CH-GING biomaterial can provide the properties not found in CH matrix [40]. In fact,

due to its similarity to collagen, GEL can enhance cell adhesion, differentiation, and proliferation. Additionally, GEL provides ample surface area for chondrocyte attachment, matrix production, and accumulation and biocompatibility. Furthermore, GEL-CH-GING was biodegradable, with a degradation rate that aligns with the pace of chondrogenesis.

The biomechanical behaviour of GEL-CH-GING composite enhanced the insufficient mechanical qualities of cartilage caused by irradiation mainly on proteoglycan production. In fact, it is a major component of cartilage matrix production, playing a crucial role in providing osmotic resistance to withstand compressive forces [41, 42]. After 60 days, no significant difference was observed between the experimental specimens and the native cartilage. In the beginning of cartilage remodelage, clusters of neocartilage were observed. Then, the biomaterial gradually degraded as the tissues continued to develop, mature, and form relatively homogeneous cartilage. By 60 days, mature chondrocytes were observed embedded in lacunae within the tissue-engineered cartilage.

The inhibition of oxidative damage by incorporation of strong antioxidants such as GING extract into GEL and CH matrix becomes an attractive therapeutic strategy, and the present formulated biomaterial may predict an expected clinical effect for osteocartilagenous tissue disorder following radiation-induced complications.

## 5. CONCLUSION

Overall, this study demonstrated that GEL-CH-GING composite could protect osteochondral tissue, enhance the biomechanical property, considerably ameliorate oxidative stress balance and alleviate the destructive effects of ionizing radiation. Thus, the synthesised composite is useful as a radioprotective for osteocartilagenous tissue. These beneficial effects of ginger may be due to its antioxidant properties. It may be considered as a natural product to prevent osteochondral cartilage destruction in the clinical setting.

## ACKNOWLEDGMENTS

The researcher(s) would like to thank the Deanship of Scientific Research, Qassim

University for funding the publication of this project.

## REFERENCES

- [1] Jebahi, S., Saoudi, M., Farhat, L., Oudadesse, H., Rebai, T., Kabir, A., El Feki, A., & Keskes, H., "Effect of novel curcumin-encapsulated chitosan-bioglass drug on bone and skin repair after gamma radiation: experimental study on a Wistar rat model". *Cell biochemistry and function*, 2015, 33(3), 150–159. <https://doi.org/10.1002/cbf.3098>
- [2] Saintigny, Y., Cruet-Hennequart, S., Hamdi, D.H., Chevalier, F., & Lefaix, JL., "Impact of therapeutic irradiation on healthy articular cartilage". *Radiation research*, 2015, 183(2), 135–146. <https://doi.org/10.1667/RR13928.1>
- [3] Zahan, O.M., Serban, O., Gherman, C., & Fodor, D. "The evaluation of oxidative stress in osteoarthritis". *Medicine and pharmacy reports*, 2020, 93(1), 12–22. <https://doi.org/10.15386/mpr-1422>
- [4] Dai, S., Wen, Y., Luo, P., Ma, L., Liu, Y., Ai, J., & Shi, C., "Therapeutic implications of exosomes in the treatment of radiation injury". *Burns & trauma*, 2022, 10, tkab043. <https://doi.org/10.1093/burnst/tkab043>
- [5] Choi, S.Y., Kim, S., & Park, K.M., "Initial Healing Effects of Platelet-Rich Plasma (PRP) Gel and Platelet-Rich Fibrin (PRF) in the Deep Corneal Wound in Rabbits". *Bioengineering (Basel, Switzerland)*, 2022, 9(8), 405. <https://doi.org/10.3390/bioengineering9080405>
- [6] Cinat, D., Coppes, R.P., & Barazzuol, L., "DNA Damage-Induced Inflammatory Microenvironment and Adult Stem Cell Response". *Frontiers in cell and developmental biology*, 2021, 9, 729136. <https://doi.org/10.3389/fcell.2021.729136>
- [7] Jebahi, S., Odadesse, H., Saoudi, M., Kallabi, F., Pellen, P., Rebai, T., El Feki, A., Keskes, H., "Cytocompatibility, gene-expression profiling, apoptotic, mechanical and (29) Si, (31)P solid-state nuclear magnetic resonance studies following treatment with a bioglass-

chitosan composite". *Biotechnology letters*, 2014, 36(12), 2571–2579. <https://doi.org/10.1007/s10529-014-1633-z>

[8] Jebahi, S., Ben Salah, G., Saoudi, M., Besaleh, S., Oudadesse, H., Mhadbi, M., Rebai, T., Keskes, H., El Feki, A., "Genotoxicity effect, antioxidant and biomechanical correlation: experimental study of agarose-chitosan bone graft substitute in New Zealand white rabbit model". *Proceedings of the Institution of Mechanical Engineers. Part H, Journal of engineering in medicine*, 2014, 228(8), 800–809. <https://doi.org/10.1177/0954411914547247>

[9] Jebahi, S., Oudadesse, H., Ben Salah, G., Saoudi, M., Mesadhi, S., Rebai, T., Keskes, H., El Feki, A., and El Feki, H., "Chitosan-Based Bioglass Composite for Bone Tissue Healing: Oxidative Stress Status and Antiosteoporotic Performance in Ovariectomized Rat Model". *Korean Journal of Chemical Engineering*, 2014, 31, 1616–1623. <https://doi.org/10.1007/s11814-014-0072-9>

[10] Jebahi, S., Bessalah, S., Zagrouba, M., Hajji, S., Raoufi, A., Hidouri, M., "The Effect of Gamma Rays on Gelatin/Chitosan Wound Dressing Physico-Chemical and Biological Properties". *Iranian Journal of Materials Science and Engineering*, 2022, 19, 2.

[11] Jebahi, S., Bessalah, S., Raouafi, A., Hajji, S., Keskes, H., Hidouri, M., "Novel bioactive adhesive dressing based on gelatin/chitosan cross-linked cactus mucilage for wound healing". *The International journal of artificial organs*, 2022, 45(10), 857–864. <https://doi.org/10.1177/03913988221114158>

[12] Martinez-Garcia, F.D., Van Dongen, J.A., Burgess, J.K., Harmsen, M.C., "Matrix Metalloproteases from Adipose Tissue-Derived Stromal Cells Are Spatiotemporally Regulated by Hydrogel Mechanics in a 3D Microenvironment". *Bioengineering* (Basel, Switzerland), 2022, 9(8), 340. <https://doi.org/10.3390/bioengineering9080340>

[13] Sulaiman, S.B., Idrus, R., Hwei, N.M., "Gelatin Microsphere for Cartilage Tissue Engineering: Current and Future Strategies". *Polymers*, 2020, 12(10), 2404. <https://doi.org/10.3390/polym12102404>

[14] Bessalah, S., Jebahi, S., Raoufi, A., Faraz, A., Zagrouba, M., Hammadi, M., "Physicochemical Evaluation and in Vitro Hemocompatibility of Goat Gelatin: Bioactive Dressing to Promote Wound Healing". *Iranian Journal of Materials Science and Engineering*, 2022, 19(2). <https://doi.org/10.22068/ijmse.2599>

[15] Li, P., Wu, G., "Roles of dietary glycine, proline, and hydroxyproline in collagen synthesis and animal growth". *Amino acids*, 2018, 50(1), 29–38. <https://doi.org/10.1007/s00726-017-2490-6>

[16] Mao, Q.Q., Xu, X.Y., Cao, S.Y., Gan, R.Y., Corke, H., Beta, T., Li, H., B., "Bioactive Compounds and Bioactivities of Ginger (*Zingiber officinale Roscoe*)". *Foods* (Basel, Switzerland), 2019, 8(6), 185. <https://doi.org/10.3390/foods8060185>

[17] Leyva-López, N., Gutierrez-Grijalva, E.P., Ambriz-Perez, D.L., Heredia, J.B., "Flavonoids as Cytokine Modulators: A Possible Therapy for Inflammation-Related Diseases". *International journal of molecular sciences*, 2016, 17(6), 921. <https://doi.org/10.3390/ijms17060921>

[18] Buege, J.A., Aust, S.D., "Microsomal lipid peroxidation". *Methods Enzymol.*, 1984, 105, 302–310.

[19] Marklund, S., Marklund, G., "Involvement of the superoxide anion radical in the autoxidation of pyrogallol and convenient assay for superoxide dismutase". *Eur J Biochem.*, 1975, 47, 469–474.

[20] Pagila, D.E., "Valentine WN. Studies on the quantitative and qualitative characterization of erythrocyte glutathione peroxidase". *J Lab Clin Med.*, 1967, 70, 158–169.

[21] Aebi, H., "Catalase in vitro". *Methods Enzymol.* 1984, 105, 121–126.

[22] Lowry, O.H., Rosebrough, N.J., Farr, A.L., et al. "Protein measurement with Folin phenol reagent". *J Biol Chem.* 1951, 193, 265–275.

[23] Schenk, R.K., Merz, W.A., Müller, J.A., "Quantitative histological study on bone resorption in human cancellous bone". *Acta Anat.* 1969, 74, 44–53.

[24] Ahn, J.J., Akram, K.J.D., Kwon, J.H., "Investigation of Different Factors

Affecting the Electron Spin Resonance-based Characterization of Gamma-irradiated Fresh, White, and Red Ginseng". *Journal of ginseng research*, 2012, 36(3), 308–313.  
<https://doi.org/10.5142/jgr.2012.36.3.308>

[25] Chetouani, A., Elkolli, M.M., Bounekhel, M., Benachour, D., "physicochemical characterization of gelatin- cmc composite edibles films from polyion-complex hydrogels". *J. Chil. Chem. Soc.* 2014, 59(1), 2279-2283.

[26] Kumar, S., Koh, J., "Physiochemical, Optical and Biological Activity of Chitosan-Chromone Derivative for Biomedical Applications". *International Journal of Molecular Sciences*, 2012, 13(5), 6102–6116.

[27] Lei, H., Wei, Q., Wang, Q., Su, A., Xue, M., Liu, Q., Hu, Q., "Characterization of ginger essential oil/palygorskite composite (GEO-PGS) and its anti-bacteria activity". *Materials science & engineering. C. Materials for biological applications*, 2017, 73, 381–387. <https://doi.org/10.1016/j.msec.2016.12.093>

[28] Chen, J., Li, J., Li, Z., Yi, R., Shi, S., Wu, K., Li, Y., Wu, S., "Physicochemical and functional properties of type I collagens in red stingray (*Dasyatis akajei*)". *skin. Mar. Drugs*, 2019, 17, 558.

[29] Abral, H., Ariksa, J., Mahardika, M., Handayani, D., Aminah, I., Sandrawati, N., Sugiarti, E., Muslimin, A.N., Rosanti, S.D., "Effect of heat treatment on thermal resistance, transparency and antimicrobial activity of sonicated ginger cellulose film". *Carbohydrate polymers*, 2020, 240, 116287.  
<https://doi.org/10.1016/j.carbpol.2020.116287>

[30] Yan, H., Li, P.H., Zhou, G.S., Wang, Y.J., Bao, B.H., Wu, Q.N., Huang, S.L., Rapid and practical qualitative and quantitative evaluation of non-fumigated ginger and sulfur-fumigated ginger via Fourier-transform infrared spectroscopy and chemometric methods. *Food chemistry*, 2021, 341(1), 128241. <https://doi.org/10.1016/j.foodchem.2020.128241>

[31] Jan, R., Gani, A., Masarat, D.M., Bhat, N.A., "Bioactive characterization of ultrasonicated ginger (*Zingiber officinale*) and licorice (*Glycyrrhiza Glabra*) freeze dried extracts". *Ultrasonics sonochemistry*, 2022, 88, 106048. <https://doi.org/10.1016/j.ultsonch.2022.106048>

[32] Saoudi, M., Jebahi, S., Jamoussi K., Ben Salah, G., Kallel, C., El Feki, A., "Haematological and biochemical toxicity induced by methanol in rats: ameliorative effects of *Opuntia vulgaris* fruit extract". *Human & experimental toxicology*, 2011, 30(12), 1963–1971. <https://doi.org/10.1177/0960327111403175>

[33] Saïdi, S.A., Abdelkafi, S., Jbahi, S., van Pelt, J., El-Feki, A., "Temporal changes in hepatic antioxidant enzyme activities after ischemia and reperfusion in a rat liver ischemia model: effect of dietary fish oil". *Human & experimental toxicology*, 2015, 34(3), 249–259. <https://doi.org/10.1177/0960327114531991>

[34] Sharifi-Rad, M., Varoni, E.M., Salehi, B., Sharifi-Rad, J., Matthews, K.R., Ayatollahi, S.A., Kobarfard, F., Ibrahim, S.A., Mnayer, D., Zakaria, Z.A., Sharifi-Rad, M., Yousaf, Z., Iriti, M., Basile, A., Rigano, D., "Plants of the Genus *Zingiber* as a Source of Bioactive Phytochemicals: From Tradition to Pharmacy". *Molecules* (Basel, Switzerland), 2017, 22(12), 2145. <https://doi.org/10.3390/molecules22122145>

[35] Jebahi, S., Oudadesse, H., Feki, H., Rebai, T., Keskes, H., Pascal, P., El Feki, A., "Antioxidative/oxidative effects of strontium-doped bioactive glass as bone graft in vivo assays in castrated rats". *Journal of applied biomedicine*, 2012, 10, 195–209.

[36] Lee, W.H., Sonntag, W.E., Mitschelen, M., Yan, H., Lee, Y.W., "Irradiation induces regionally specific alterations in pro-inflammatory environments in rat brain". *International journal of radiation biology*, 2010, 86(2), 132–144. <https://doi.org/10.3109/09553000903419346>

[37] Wojdasiewicz, P., Poniatowski, ŁA., Szukiewicz, D., "The role of inflammatory and anti-inflammatory cytokines in the pathogenesis of osteoarthritis". *Mediators of inflammation*, 2014, 561459. <https://doi.org/10.1155/2014/561459>

- [38] Wei, Z., Zhang, G., Cao, Q., Zhao, T., Bian, Y., Zhu, W., Weng, X., "Recent Developments and Current Applications of Organic Nanomaterials in Cartilage Repair". *Bioengineering* (Basel, Switzerland), 2022, 9(8), 390. <https://doi.org/10.3390/bioengineering9080390>
- [39] Jebahi, S., Oudadesse, H., Bui, X.V., Keskes, H., Rebai, T., El Feki, A., El Feki, H., "Repair of bone defect using bioglass-chitosan as a pharmaceutical drug: An experimental study in an ovariectomised rat model". *African Journal of Pharmacy and Pharmacology*, 2012, 6(16), 1276-1287.
- [40] Han, E.H., Chen, S.S., Klisch, S.M., Sah, R.L., "Contribution of proteoglycan osmotic swelling pressure to the compressive properties of articular cartilage". *Biophysical journal*, 2011, 101(4), 916-924. <https://doi.org/10.1016/j.bpj.2011.07.006>
- [41] Wu, C.L., Harasymowicz, N.S., Klimak, M.A., Collins, K.H., Guilak, F., "The role of macrophages in osteoarthritis and cartilage repair". *Osteoarthritis and cartilage*, 2020, 28(5), 544-554. <https://doi.org/10.1016/j.joca.2019.12.007>
- [42] Van Boxtel, J., Vonk, L.A., Stevens, H.P., van Dongen, J.A., "Mechanically Derived Tissue Stromal Vascular Fraction Acts Anti-inflammatory on TNF Alpha-Stimulated Chondrocytes In Vitro". *Bioengineering* (Basel, Switzerland), 2022, 9(8), 345. <https://doi.org/10.3390/bioengineering9080344>